

DAMTP 96-45

ϕ^4 Kinks - Gradient Flow and Dynamics

N. S. Manton* and H. Merabet†

*Department of Applied Mathematics and Theoretical Physics, University of Cambridge
Cambridge CB3 9EW, United Kingdom*

May 1996

Abstract

The symmetric dynamics of two kinks and one antikink in classical (1+1)-dimensional ϕ^4 theory is investigated. Gradient flow is used to construct a collective coordinate model of the system. The relationship between the discrete vibrational mode of a single kink, and the process of kink-antikink pair production is explored.

*e-mail address: N.S.Manton@damtp.cam.ac.uk

†e-mail address: M.Houari@damtp.cam.ac.uk

1 Introduction

One of the more challenging problems in non-integrable soliton dynamics is to find a collective coordinate model of the dynamics. In some theories there is a moduli space of exact multi-soliton static solutions, and the soliton dynamics at low energy is modelled by geodesic motion on the moduli space [10]. In exactly integrable models, like the sine-Gordon model, one can exactly compute what happens in a multi-soliton or multi-soliton-antisoliton process. There is no energy loss to radiation in these processes, and solitons do not annihilate antisolitons in a collision.

In ϕ^4 theory on a line [12], things are different. ϕ^4 theory is a nonlinear, Lorentz invariant, scalar field theory which is not integrable. The field $\phi(x, t)$ has kinetic energy

$$T = \int_{-\infty}^{\infty} \frac{1}{2} \dot{\phi}^2 dx \quad (1.1)$$

and potential energy

$$V = \int_{-\infty}^{\infty} \left(\frac{1}{2} \phi'^2 + \frac{1}{2} (\phi^2 - 1)^2 \right) dx . \quad (1.2)$$

The Lagrangian is $L = T - V$, and this leads to the field equation

$$\ddot{\phi} - \phi'' + 2\phi (\phi^2 - 1) = 0. \quad (1.3)$$

There are two vacua, $\phi = \pm 1$. There are also two types of solitons, called kinks and antikinks. A kink interpolates between -1 and 1 as x increases, and an antikink does the reverse. Eq.(1.3) has static solutions

$$\phi_K(x - a) = \tanh(x - a) \quad \text{and} \quad \phi_{\bar{K}}(x - b) = -\tanh(x - b), \quad (1.4)$$

where ϕ_K and $\phi_{\bar{K}}$ are the kink and the antikink respectively. They have potential energy (rest mass) $\frac{4}{3}$. The parameter a (b) denotes the centre of the kink (antikink). These solutions can be Lorentz boosted to an arbitrary speed $v < c$ (where the speed of light $c = 1$ in our units). There are non-static field configurations with several kinks and antikinks, but kinks and antikinks must alternate along the line. A neighbouring kink and antikink can annihilate into small amplitude oscillations of the field ϕ – interpreted as radiation. Also, in suitable circumstances, a kink-antikink pair can be produced.

There has been a substantial investigation of kink-antikink dynamics (see, e.g. ref.[5]). If a kink and antikink approach from infinity, starting with any speed much less than the speed of light, they will annihilate into radiation. In higher speed collisions, what happens depends sensitively on the speed.

We have investigated a different process, which appears to be better suited to a collective coordinate analysis. This is the symmetric motion of a configuration of two kinks and an antikink, which we denote $K\bar{K}K$. We consider fields which possess the reflection symmetry

$$\phi(x) = -\phi(-x) \quad (1.5)$$

at all times, and for which $\phi \rightarrow 1$ as $x \rightarrow \infty$. This allows, among other things, for there to be kinks centred at $\pm a$, and an antikink at the origin. A field of this type can evolve into a single kink plus radiation, but the radiation is not emitted very rapidly, as we shall show.

An interesting and important feature of ϕ^4 kink dynamics is that a single kink has a normalizable discrete vibrational mode. The discrete mode deforms a static kink at the origin to the form

$$\phi(x) = \phi_K(x) + A \eta_D(x) \quad \text{with} \quad \eta_D(x) = \frac{\sinh(x)}{\cosh^2(x)}, \quad (1.6)$$

where, in the linearized approximation, the amplitude A oscillates with frequency $\omega_0 = \sqrt{3}$. In comparison, the continuum radiation modes have frequencies $\omega > 2$. Fields of the form (1.6) have the reflection symmetry (1.5). When $A \simeq -2$, the field (1.6) looks rather like a $K\bar{K}K$ configuration with the kinks close together. In fact it is possible to smoothly interpolate between a $K\bar{K}K$ configuration with the kinks well-separated, and a single kink, via fields of the approximate form (1.6).

2 Gradient Flow

We recall that a natural (finite-dimensional) Lagrangian system on a configuration space \mathcal{C} has a Lagrangian of the form [2]

$$L(\dot{\mathbf{y}}, \mathbf{y}) = T(\dot{\mathbf{y}}, \mathbf{y}) - V(\mathbf{y}), \quad \text{where} \quad T(\dot{\mathbf{y}}, \mathbf{y}) = \frac{1}{2} g_{ij}(\mathbf{y}) \dot{y}^i \dot{y}^j. \quad (2.1)$$

Here, y^i are arbitrary coordinates on \mathcal{C} , and $g_{ij}(\mathbf{y})$ can be interpreted as a Riemannian metric on \mathcal{C} . The Euler-Lagrange equation is

$$\frac{d}{dt}(g_{ij}(\mathbf{y}) \dot{y}^j) = -\frac{\partial V}{\partial y^i} \quad (2.2)$$

whereas the gradient flow equation is

$$g_{ij}(\mathbf{y}) \dot{y}^j = -\frac{\partial V}{\partial y^i}. \quad (2.3)$$

The gradient flow is orthogonal to the contours of the potential V – the notion of orthogonality requires a metric – and in the direction of decreasing V . If \mathbf{y}_0 is a saddle point of V , then the unstable manifold of \mathbf{y}_0 is defined as the union of all the gradient flow curves that descend from \mathbf{y}_0 .

If the configuration space is Euclidean, and y^i are Cartesian coordinates, then the gradient flow equation is obtained from the Euler-Lagrange equation by replacing second time derivatives by first time derivatives. ϕ^4 field theory can be thought of as an infinite-dimensional Lagrangian system whose configuration space \mathcal{C} is the space of fields $\{\phi(x)\}$ at a given time.

The simple form of the kinetic energy expression (1.1) implies that \mathcal{C} is Euclidean, with the Riemannian distance between fields $\phi(x)$ and $\phi(x) + \delta\phi(x)$ being the square root of

$$\int_{-\infty}^{\infty} (\delta\phi(x))^2 dx . \quad (2.4)$$

The gradient flow equation is therefore obtained from eq.(1.3) simply by replacing $\ddot{\phi}$ by $\dot{\phi}$, giving

$$\dot{\phi} = \phi'' - 2\phi (\phi^2 - 1). \quad (2.5)$$

In ref.[11] it was proposed that a collective coordinate model of multi-soliton dynamics could be systematically obtained using the method of gradient flow. The collective coordinate dynamics takes place on the unstable manifold of a suitable static solution of the field equations. The solution could either be a genuine localised one, representing some static, but unstable, configuration of coincident solitons, or a virtual solution representing static solitons at infinite separation. A similar idea - “the valley method” - has been used for defining instanton-antiinstanton configurations, and using these to investigate tunneling phenomena in quantum mechanics and quantum field theory [4].

The unstable manifold acquires a metric and potential from the configuration space of which it is a submanifold. These define a Lagrangian for dynamical motion on the unstable manifold, leading to an Euler-Lagrange equation of the form (2.2). This reduced dynamical system is the collective coordinate model for the soliton dynamics. Any set of coordinates on the unstable manifold can be regarded as collective coordinates for the solitons, although there may be a preferred choice if the solitons are well-separated. A solution of the Euler-Lagrange equation on the unstable manifold is not, in general, identical with any solution of the original field equations, but it may provide an approximation.

The reduced system should be particularly useful if the potential energy function does not vary much over the unstable manifold, that is, if the static forces between solitons are weak (but nonvanishing), so large kinetic energies are not generated. The unstable manifold is then an almost flat valley in the field configuration landscape, and the motion on it at modest speeds is expected to be a good approximation to the true field dynamics. This is because motion orthogonal to the valley is not readily generated. However, this has not really been demonstrated analytically, nor tested numerically. In the limiting case of there being no potential, the reduced dynamics is geodesic motion, and in this case it has been proved by Stuart that the slow motion of solitons is well approximated by the reduced dynamics [14].

The gradient flow in field theories with solitons has been investigated in detail in one or two cases. Demoulini and Stuart have studied the gradient flow in the two-dimensional abelian Higgs model [6], whose solitons are magnetic flux vortices, proving the global existence of gradient flow curves, and obtaining some insight into the relevant unstable manifolds. Waindzoch and Wambach have studied the gradient flow in the two-Skyrmion sector of Skyrme’s soliton model of nucleons [15], the geometry of which was discussed in [3], and have numerically (partially) constructed an unstable manifold which should model the two-Skyrmion dynamics. Also, there has been a detailed study of the gradient flow equation (2.5) for ϕ defined

on a finite interval [7]. It has been shown that the unstable manifold of the simplest unstable solution on the interval, namely $\phi = 0$, completed with the unstable manifolds of lower energy solutions, is a global attractor for eq.(2.5). However, there has been no comparison made between the solutions of the dynamical equation (1.3) and the dynamical motion on the unstable manifold. This example of ϕ^4 theory on an interval shows that an unstable manifold can have a non-smooth boundary (see Fig. 8.5 in ref. [7]). For an unstable manifold to be useful for modelling multi-soliton dynamics, and especially quantized soliton dynamics, it is important that the manifold has no boundary at all. The vortex and Skyrme examples appear to satisfy this requirement. Mathematically, it is not at all clear in what circumstances an infinite-dimensional gradient flow system has a smooth, finite-dimensional global attractor without boundary.

Here, we use the gradient flow method to construct a collective coordinate model for the $K\bar{K}K$ system of ϕ^4 theory, with the imposed reflection symmetry (1.5). We shall compare the collective coordinate dynamics with the dynamics defined by the field equation (1.3). Because kink-antikink annihilation occurs in $K\bar{K}K$ dynamics, the kinetic energy can become large. Nevertheless, as we shall see, the reduced dynamical system appears to be a useful approximation.

Because of the reflection symmetry, the $K\bar{K}K$ system is modelled by a one-dimensional unstable manifold. It consists of the field configurations $\phi(x)$, parametrized by $-\infty < t < \infty$, occurring in the solution of the gradient flow equation (2.5) which descends from a $K\bar{K}K$ configuration, with kinks at $\pm\infty$ and an antikink at the origin, to a single kink at the origin. This solution approaches the single kink tangent to its discrete mode. The collective coordinate can be identified either with the separation of the kinks from the antikink, while this is large, or with the discrete mode amplitude, while this has a modest or small negative value.

The unstable manifold is infinitely long. At the top end, where there are kinks at infinite separation, the potential energy is 4 (three times the kink rest mass). At the bottom, where there is a single kink, the potential energy is $\frac{4}{3}$. Most of the unstable manifold consists of well-separated $K\bar{K}K$ configurations, with kinks at $\pm a$ and an antikink at the origin. We cannot write down the exact form of the fields satisfying (2.5), but for $a \gg 1$ an exponentially accurate approximation is given by the product form

$$\phi = -\phi_K(x+a) \phi_{\bar{K}}(x) \phi_K(x-a) , \quad (2.6)$$

with a a function of time. To a sufficiently good approximation, the Lagrangian for such fields is $\frac{4}{3}\dot{a}^2 + 32e^{-2a} - 4$, since there are two kinks moving with velocities $\pm\dot{a}$, and the interaction potential of a $K\bar{K}$ pair separated by a is $-16e^{-2a}$ if a is large [9]. The gradient flow equation therefore reduces to

$$\dot{a} = -24e^{-2a} \quad (2.7)$$

whose integral is $e^{2a} = -48t + \text{const.}$ We have verified this by taking the initial data (2.6) with $a = 5$, and evolving it numerically with the gradient flow equation (2.5) until the three zeros of ϕ are at $x = \pm 4$ and $x = 0$. The time this takes is very close to $\frac{1}{48}(e^{10} - e^8) \simeq 397$, which is a very long time compared with the period of the discrete mode oscillation.

For $a < 4$, the expression (2.6) fails to be a good approximation for the fields on the unstable manifold, so we have integrated (2.5) numerically, starting at $t = 0$ with initial data (2.6) with $a = 4$. We find that after a finite time the $K\bar{K}K$ configuration annihilates into a deformed single kink. An exact annihilation time can be defined as the time when the three zeros of ϕ coalesce into one. Equivalently, this is when ϕ' is zero at the origin. (ϕ' is negative before this time and positive afterwards.) The annihilation time, for our initial data, is $t = 59.64$. By integrating (2.7) and finding when $a = 0$, one may estimate the annihilation time to be $t = \frac{1}{48}(e^8 - 1) \simeq 62$.

As t increases further, the field configuration rapidly approaches the single kink, and it does so tangent to the discrete mode, since this is the lowest frequency mode of vibration around the kink. So the field becomes well approximated by the form (1.6), with an amplitude $A(t)$ tending to zero. Even at the annihilation time, the field (1.6) with $A = -1$ is a reasonable approximation, since for this value of A , ϕ' vanishes at the origin. The asymptotic behaviour of $A(t)$ is given by calculating from (1.1) and (1.2) the kinetic and potential energies for fields of the form (1.6). These are, respectively,

$$T(A) = \frac{1}{3}\dot{A}^2 \quad (2.8)$$

and

$$V(A) = \frac{4}{3} + A^2 + \frac{\pi}{8}A^3 + \frac{2}{35}A^4, \quad (2.9)$$

giving a gradient flow equation

$$\frac{2}{3}\dot{A} = -2A - \frac{3\pi}{8}A^2 - \frac{8}{35}A^3. \quad (2.10)$$

As $t \rightarrow \infty$, A decays like e^{-3t} , the coefficient being the square of the discrete mode frequency.

Our numerical solution of the gradient flow equation was obtained using a predictor-corrector finite difference scheme. Since this is an implicit scheme, there is no stability restriction on $\Delta t/\Delta x^2$ (see [1]). The resulting tridiagonal linear system is solved explicitly using the Thomas algorithm. Our space-time domain is defined on $-10 \leq x \leq 10$ and $0 \leq t \leq 65$ in space and time steps of 0.02 and 0.005 respectively. Fig. 1 shows the field ϕ at the initial time and various subsequent times. The annihilation process occurs at $t \sim 60$. Fig. 2 shows the potential energy as a function of time. The rapid decrease occurs close to the annihilation time.

The unstable manifold stops abruptly at the single kink. It is desirable to define a valley which smoothly continues it. The valley continuation needs to approach the single kink tangent to the discrete mode from the opposite direction. The best continuation we can think of is the set of fields (1.6) with $A > 0$. With this ansatz, the potential energy in the valley, and its first, second and third derivatives, are all continuous at the single kink, but the fourth derivative is probably discontinuous. The positive value of A for which the potential energy expression (2.9) has value 4 is 1.3.

Any field $\phi(x)$, with the reflection symmetry and boundary conditions we are assuming, has a decomposition

$$\phi(x) = \phi_K(x) + A \eta_D(x) + \eta(x) \quad (2.11)$$

where $\eta(x)$ is a superposition of continuum modes orthogonal to the discrete mode $\eta_D(x)$. We can calculate the amplitude of the discrete mode A by projection

$$A = \frac{3}{2} \int_{-\infty}^{\infty} (\phi(x) - \phi_K(x)) \eta_D(x) dx . \quad (2.12)$$

In the valley, A varies between $-3\pi/2$ and ∞ . The first number is calculated using (2.12) with $\phi(x)$ a $K\bar{K}K$ configuration with kinks at infinite separation, and its finite value implies that the tangent to the unstable manifold is asymptotically orthogonal to the discrete mode (both metrically, and in the usual sense of integration). The $K\bar{K}K$ half of the valley is therefore curved, turning a right angle along its length. The half of the valley defined using the ansatz (1.6), with A positive, is straight.

Along the valley, the arc length s is the only intrinsic geometrical quantity. Suppose $s = 0$ at the bottom, with s positive in the $K\bar{K}K$ half of the valley. Let $V(s)$ be the potential energy in the valley, as a function of arc length. The intrinsic gradient flow equation is

$$\dot{s} = -\frac{dV}{ds} \quad (2.13)$$

and in the $K\bar{K}K$ half of the valley this must give the same dependence of V with time, as the field gradient flow equation. Eq. (2.13) implies

$$\frac{dV}{dt} = - \left(\frac{ds}{dt} \right)^2 . \quad (2.14)$$

We have taken our numerically obtained $V(t)$ and integrated $\sqrt{-\dot{V}}$ to find $s(t)$, and hence determined s and $V(s)$ along the curved half of the valley. The kinetic energy expression (2.8) for a field of the form (1.6) implies that for small s , we may identify $s = -\sqrt{\frac{2}{3}}A$. For large positive s we may identify $ds = \sqrt{\frac{8}{3}}da$. Numerically we estimate that for large a , $s = \sqrt{\frac{8}{3}}a - 1.18$. The arc length along the straight half of the valley is exactly $s = -\sqrt{\frac{2}{3}}A$, and using this relation we can easily convert the potential function (2.9) into a function of s . Fig. 3 shows the potential function $V(s)$ in both halves of the valley. If we use the discrete mode ansatz (1.6) also for $s > 0$ we get the dashed curve in the Figure, which is not a bad approximation for $|A| \leq 2$. Note the asymmetry of the potential, due to the A^3 term in V .

3 Dynamics

The one-dimensional dynamical system

$$L = \frac{1}{2}\dot{s}^2 - V(s) , \quad (3.1)$$

with $V(s)$ as shown in Fig. 3, is our collective coordinate model for the dynamics of the $K\bar{K}K$ system. It predicts that for energies $\frac{4}{3} < E < 4$, there is a nonlinear oscillatory behaviour. For $E > 4$ it predicts that two kinks can approach from infinity and annihilate an antikink at the origin, with the kinetic energy being captured by the discrete mode of the kink that remains; then the process reverses and $K\bar{K}K$ reform. The model also predicts that if the initial data is of the form (1.6) with $A = 0$ and $|\dot{A}| > 2\sqrt{2}$, then a $K\bar{K}K$ configuration will form, and the kinks move off to infinity. (The more direct process is with \dot{A} initially negative.)

We do not expect the field dynamics to be exactly along the part of the valley defined by the gradient flow, since, as we have shown, the valley is extrinsically curved. However, we expect the motion along the valley to be a guide, rather like the bottom of a bobsleigh run is a guide to the bobsleigh trajectories. As the valley turns, so the dynamical motion must climb up the side of the valley to be forced round the corner. We also expect some vibrational motion orthogonal to the valley to be generated.

We have numerically studied the field dynamics of the $K\bar{K}K$ system, given by eq.(1.3). The integration is performed using a second-order three level implicit formula. As for the gradient flow case, this scheme is stable for any value of $\Delta t/\Delta x$ provided that the three level parameter is greater than 1/4 (see [1]). Our space-time domain is defined on $-20 \leq x \leq 20$ and $0 \leq t \leq 60$ in space and time steps of 0.02 and 0.015 respectively. We have considered two kinds of initial data.

First, we have taken the initial data (2.6) with $a = 4$ and with $\dot{\phi} = 0$. The initial potential energy is very close to 4. We observe (see Fig. 4) that the two kinks approach the antikink at the origin and annihilate, producing a kink with an excited discrete mode. The system oscillates back to $K\bar{K}K$, but the separation is reduced. The motion continues, essentially as a large amplitude nonlinear oscillation of the discrete mode. Energy is slowly transferred to radiation modes, which is emitted symmetrically and escapes to infinity.

Fig. 5 shows the potential energy and total energy as a function of time. Total energy is conserved until $t \simeq 40$, which is when radiation first arrives at the boundary of the simulation interval. Our boundary conditions absorb this radiation. Notice that at $t = 18.75$, after one oscillation of the field, the potential energy is about 1.38 which is very close to $\frac{4}{3}$, the energy of the static kink, so the field dynamics passes very close to the bottom of the valley at that time. Notice also the very long time during which the system oscillates with frequency just less than $\sqrt{3}$, and the slow production of radiation. In one period of oscillation the potential energy has two minima but these have unequal spacing in time. We have estimated theoretically the rate of energy loss to radiation from the oscillating discrete mode, and this agrees well with what we see numerically (see Appendix A).

Fig. 6 shows $A(t)$, the amplitude of the discrete mode calculated using eq.(2.12), for our dynamical field $\phi(x, t)$. If the $K\bar{K}K$ system moved exactly in the valley, with total energy less than 4, A would oscillate without loss of amplitude. We see in Fig. 6 that A oscillates with slowly decreasing amplitude. The asymmetry of the oscillation can be understood from the asymmetry of the potential about the bottom of the valley. Note that the first time A is positive, it reaches 1.15. This is close to the value 1.3 predicted for motion in the valley

with total energy 4. Fig. 7 shows the field ϕ obtained dynamically, at the moment when A as defined by (2.12) is 1.15, compared to the ansatz (1.6) with $A = 1.15$.

Second, we have considered the initial data $\phi = \phi_K(x)$, $\dot{\phi} = -C\eta_D(x)$, that is, a single kink with its discrete mode excited. This motion starts at the bottom of the valley and tangent to the valley bottom, and although the valley is curved, we expect the motion to be guided round the curve, so that a $K\bar{K}K$ configuration will be produced if C is sufficiently large.

If $C = 2\sqrt{2}$, then the initial kinetic energy is $\frac{8}{3}$, which is just sufficient to produce a kink-antikink pair. In practice, some energy goes into radiation, and this value of C is not large enough. The critical value for kink-antikink pair production is $C \simeq 3.06$. Here, two kinks reach the boundary of our region $-20 \leq x \leq 20$, leaving an antikink at the origin, and since the forces between the kinks and the antikink are negligible at these separations, the kinks would presumably travel to infinity. Since 3.06 is not much greater than $2\sqrt{2}$, we see that exciting the discrete mode of a single kink is an efficient mechanism for producing a $K\bar{K}$ pair. As C increases beyond 3.06, so the outgoing kinks have higher speed, and there is also more radiation. Energetically, two $K\bar{K}$ pairs could be produced when $C = 4$ but in practice, more energy is needed, and the production first occurs when $C = 4.71$.

Figs. 8 and 9 show the field $\phi(x, t)$ for $-20 \leq x \leq 20$ and $0 \leq t \leq 60$ with $C = 3.06$. One can see how the discrete mode evolves into the $K\bar{K}K$ system. The small amount of associated radiation is visible too. Fig. 10 shows the creation of two $K\bar{K}$ pairs when $C = 4.71$.

4 Conclusion

The $K\bar{K}K$ system with reflection symmetry is well-described by a one-dimensional reduced dynamical system with an asymmetric potential. This is quite surprising because annihilation of a kink and antikink can and does occur, releasing a large amount of energy. However, most of this energy is converted to the oscillation of the discrete mode of the remaining kink. The collective coordinate of the one-dimensional system can therefore be interpreted as the separation of the kinks from the antikink, or as the amplitude of the discrete mode, in different regions. We have defined the reduced system on one side of the minimum of the potential by gradient flow, on the other by an ansatz just involving the discrete mode, but perhaps a better ansatz is possible. The reduced dynamics is a good approximation to the full field dynamics, because the discrete mode couples quite weakly to radiation modes.

We conjecture that in other field theories, multi-soliton and soliton-antisoliton dynamics can be similarly reduced to finite-dimensional systems using gradient flow, and that discrete vibrational modes of the solitons may again play an important role. Soliton-antisoliton pair production may be associated with large amplitude excitations of the discrete modes in these other field theories. Perhaps soliton-antisoliton pair production at high temperatures can be catalysed by the presence of solitons, if these solitons have suitable discrete vibrational modes.

Appendix A

Radiation from an oscillating kink

In the linear approximation, the discrete mode of the kink oscillates harmonically with frequency $\sqrt{3}$. However, when the nonlinearity of the fields is taken into account, this mode couples to the continuum radiation modes and eventually all its energy is radiated away. We can estimate the rate at which this happens as follows.

Let us write the field ϕ as

$$\phi(x, t) = \phi_K(x) + A(t) \eta_D(x) + \eta(x, t) \quad (\text{A.1})$$

where $\phi_K(x) = \tanh(x)$ and $\eta_D(x) = \sinh(x)/\cosh^2(x)$. The function $\eta(x, t)$ represents the continuum part of the deformation of the kink, and hence is orthogonal to the discrete mode

$$\int_{-\infty}^{\infty} \eta(x, t) \eta_D(x) dx = 0. \quad (\text{A.2})$$

It is consistent to assume $\eta(x, t)$ is odd in x . If we substitute (A.1) into the field equation (1.3) we find

$$\begin{aligned} (\ddot{A} + 3A)\eta_D + \ddot{\eta} - \eta'' + (6\phi_K^2 - 2)\eta &= -6(\eta + \phi_K)\eta_D^2 A^2 \\ &\quad - 6(\eta + 2\phi_K)\eta\eta_D A \\ &\quad - 2\eta_D^3 A^3 - 6\phi_K\eta^2 - 2\eta^3 \end{aligned} \quad (\text{A.3})$$

At $\mathcal{O}(A)$, the discrete mode oscillates with frequency $\sqrt{3}$, and there is no source for η , so it is consistent to set $\eta = 0$. At $\mathcal{O}(A^2)$, there is a source for η , the term $-6\phi_K\eta_D^2 A^2$. If A is small, we may suppose that η is $\mathcal{O}(A^2)$, and we may neglect terms in (A.3) involving A^3 , η^2 , ηA , etc. The reduced system is

$$(\ddot{A} + 3A)\eta_D + \ddot{\eta} - \eta'' + (6\phi_K^2 - 2)\eta = -6\phi_K\eta_D^2 A^2 \quad (\text{A.4})$$

The source term $-6\phi_K\eta_D^2 A^2$ splits into two parts, a projection onto the discrete mode, and a projection orthogonal to this. The projection onto the discrete mode implies an anharmonic oscillation of A , but this is not a large effect and the frequency of the oscillation is unchanged to lowest order. The projection orthogonal to the discrete mode is the source for η . Fortunately the eigenfunctions of the Schrödinger operator

$$-\frac{d^2}{dx^2} + (6\phi_K^2 - 2) \quad (\text{A.5})$$

are known exactly [12], so the Green's function can be computed and the response of η to the source can be calculated by explicit integration.

The truncation (A.4) is not energy conserving. The discrete mode oscillation creates radiation but there is no backreaction on the amplitude of the discrete mode. We may calculate

the backreaction by finding the energy carried away by the radiation, and may infer the rate of decrease of the amplitude of the discrete mode, using energy conservation. Our calculation depends on the rate of energy loss being small during the period $\frac{2\pi}{\sqrt{3}}$.

Let the projection of $\phi_K \eta_D^2$ onto the discrete mode be $\alpha \eta_D$, so the orthogonal projection is $\phi_K \eta_D^2 - \alpha \eta_D$. The constant α is determined by

$$\int_{-\infty}^{\infty} \phi_K(x) \eta_D(x)^3 dx - \alpha \int_{-\infty}^{\infty} \eta_D(x)^2 dx = 0 \quad , \quad (\text{A.6})$$

implying $\alpha = \frac{3\pi}{32}$. The oscillation of the discrete mode, to $\mathcal{O}(A^2)$, therefore obeys

$$\ddot{A} + 3A + 6\alpha A^2 = 0 \quad (\text{A.7})$$

which agrees with what would be obtained, at this order, from (2.8) and (2.9). The equation for η is

$$\ddot{\eta} - \eta'' + (6\phi_K^2 - 2)\eta = 6(\alpha \eta_D - \phi_K \eta_D^2) A^2 \quad (\text{A.8})$$

Let us now assume that $A = A_0 \cos(\sqrt{3}t)$, so $A^2 = \frac{1}{2}A_0^2(\cos(2\sqrt{3}t) + 1)$. The response of η to the time-independent source is itself time-independent and carries away no energy. The important part of η is at the single frequency $2\sqrt{3}$. Let us therefore consider the equation

$$\ddot{\eta} - \eta'' + (6\phi_K^2 - 2)\eta = f(x) \exp(i\omega t) \quad (\text{A.9})$$

where $\omega > 2$. Setting $\eta(x, t) = \eta(x) \exp(i\omega t)$, we obtain

$$-\eta'' + (6\phi_K^2 - 2 - \omega^2)\eta = f(x) . \quad (\text{A.10})$$

The homogenous equation (A.10) (with $f \equiv 0$) has exact solutions [12]

$$\begin{aligned} \eta_q(x) &= (3\phi_K^2(x) - 1 - q^2 - 3iq\phi_K(x)) \exp(+iqx) \\ \eta_{-q}(x) &= (3\phi_K^2(x) - 1 - q^2 + 3iq\phi_K(x)) \exp(-iqx) \end{aligned} \quad (\text{A.11})$$

where $q = \sqrt{\omega^2 - 4}$. From the form of these solutions as $x \rightarrow \infty$, we compute the Wronskian

$$W = \eta_q(x) \eta'_{-q}(x) - \eta'_{-q}(x) \eta_{-q}(x) = -2iq(q^2 + 1)(q^2 + 4) . \quad (\text{A.12})$$

The solution of (A.10) that we want is the one with outgoing radiation. The relevant Green's function is

$$G(x, \xi) = \begin{cases} -\frac{1}{W} \eta_{-q}(\xi) \eta_q(x) & (x < \xi) \\ -\frac{1}{W} \eta_q(\xi) \eta_{-q}(x) & (x > \xi) \end{cases} . \quad (\text{A.13})$$

So the desired solution of (A.10) is

$$\eta(x) = -\frac{1}{W} \eta_{-q}(x) \int_{-\infty}^x f(\xi) \eta_q(\xi) d\xi - \frac{1}{W} \eta_q(x) \int_x^{\infty} f(\xi) \eta_{-q}(\xi) d\xi . \quad (\text{A.14})$$

We may use the asymptotic form of (A.11) to obtain the form of the solution (A.14) for large x ,

$$\eta(x) = \frac{1}{2iq(2 - q^2 - 3iq)} \exp(-iqx) \int_{-\infty}^{\infty} f(\xi) \eta_q(\xi) d\xi . \quad (\text{A.15})$$

Thus, for the source $-3A_0^2\phi_K\eta_D^2 \cos(2\sqrt{3}t)$, $\eta(x, t)$ is asymptotically

$$\eta(x, t) = \text{Re} \left(\frac{-3A_0^2}{2iq(2 - q^2 - 3iq)} \exp(i(\omega t - qx)) \int_{-\infty}^{\infty} \phi_K(\xi) \eta_D^2(\xi) \eta_q(\xi) d\xi \right) \quad (\text{A.16})$$

where $\omega = 2\sqrt{3}$ and $q = 2\sqrt{2}$. It is sufficient here to write the source as proportional to $\phi_K\eta_D^2$, since the integral of $\eta_D\eta_q$ vanishes.

Eq.(A.16) represents outward moving radiation for large x . There is similar outward radiation for large negative x . To calculate the integral in (A.16), we use the result

$$\begin{aligned} I(q) &= \int_{-\infty}^{\infty} \phi_K(\xi) \eta_D^2(\xi) (3\phi_K^2(\xi) - 1 - q^2 - 3iq\phi_K(\xi)) \exp(iq\xi) d\xi \\ &= \frac{i\pi q^2}{48 \sinh(\pi q/2)} (q^2 + 4)(q^2 - 2) . \end{aligned} \quad (\text{A.17})$$

Thus (A.16) reads now

$$\eta(x, t) = \frac{\pi q(q^2 - 2)}{32 \sinh(\pi q/2)} \sqrt{\frac{q^2 + 4}{q^2 + 1}} A_0^2 \cos(\omega t - qx - \delta) \quad (\text{A.18})$$

where δ is a phase depending on q . We are only interested in the amplitude of the radiation, not its phase. For $q = 2\sqrt{2}$ the amplitude is

$$R = \frac{\pi\sqrt{3/8}}{\sinh(\pi\sqrt{2})} A_0^2 = 0.0453 A_0^2 \quad (\text{A.19})$$

For a wave of the form $\eta = R \cos(\omega t - qx - \delta)$ the average energy flux to the right is $\frac{1}{2}R^2\omega q$, so the total energy flux away from the oscillating kink is $R^2\omega q$. The rate of energy loss by the discrete mode (averaged over a period) is

$$\frac{dE}{dt} = -(0.0453)^2 4\sqrt{6} A_0^4 = -0.020 A_0^4 . \quad (\text{A.20})$$

On the other hand, the energy of the discrete mode is $E = A_0^2$, so the rate of decay of the amplitude is given by

$$\frac{dA_0^2}{dt} = -0.020 A_0^4 \quad (\text{A.21})$$

which can be integrated to give

$$\frac{1}{A_0^2(t)} - \frac{1}{A_0^2(0)} = 0.020 (t - t_0) . \quad (\text{A.22})$$

We can calculate the decay of the discrete mode amplitude due to radiation in another way. Consider again the exact equation (A.3).

Using the orthogonality condition (A.2), we project the equation (A.3) onto the discrete mode

$$\ddot{A} + \omega_0^2 A = a_0 + a_1 A + a_2 A^2 + a_3 A^3 \quad (\text{A.23})$$

where we have defined

$$\begin{aligned} a_0 &= -3 \int_{-\infty}^{\infty} (3\phi_K + \eta) \eta^2 \eta_D dx; & a_1 &= -9 \int_{-\infty}^{\infty} (2\phi_K + \eta) \eta^2 \eta_D^2 dx \\ a_2 &= -9 \int_{-\infty}^{\infty} \eta \eta_D^3 dx - 6\alpha; & a_3 &= -3 \int_{-\infty}^{\infty} \eta_D^4 dx = -\frac{12}{35}. \end{aligned} \quad (\text{A.24})$$

Following ref.[8], and as in [13], we seek a perturbative solution for $\phi(x, t)$ of the form (A.1) with

$$\begin{aligned} A &= A^{(1)} + A^{(2)} + A^{(3)} + \dots \\ \eta &= \eta^{(1)} + \eta^{(2)} + \eta^{(3)} + \dots \end{aligned} \quad (\text{A.25})$$

and with A having period $2\pi/\tilde{\omega}$, where

$$\tilde{\omega} = \omega_0 + \omega^{(1)} + \omega^{(2)} + \dots \quad (\text{A.26})$$

At the first order, the discrete mode oscillates with the frequency $\omega_0 = \sqrt{3}$, and there is no source term for the continuum modes, so $A^{(1)} = A_0 \cos(\omega_0 t)$ and $\eta^{(1)} = 0$.

At the second order, eq.(A.23) reduces to

$$\ddot{A}^{(2)} + \omega_0^2 A^{(2)} = -6\alpha A^{(1)2} + 2\omega_0 \omega^{(1)} A_0 \cos(\omega_0 t). \quad (\text{A.27})$$

The requirement that the resonance term (at frequency ω_0) be absent implies $\omega^{(1)} = 0$, so we obtain exactly eq.(A.7). The latter displays the first anharmonic correction to the discrete mode oscillation. Writing $A^{(1)2} = \frac{1}{2}A_0^2(\cos(2\omega_0 t) + 1)$, the solution of eq.(A.27) reads

$$A^{(2)} = \frac{\alpha}{\omega_0^2} A_0^2 (\cos(2\omega_0 t) - 3). \quad (\text{A.28})$$

The correction (A.28) tells us that the main source of the asymmetric oscillation of A in Fig. 6 is the cubic term of the potential (2.9).

By expanding eq.(A.3) up to the second order in η and A , we obtain

$$\ddot{\eta}^{(2)} - \eta''^{(2)} + (6\phi_K^2 - 2)\eta^{(2)} = 6(\alpha - \phi_K \eta_D) \eta_D A^{(1)2} \quad (\text{A.29})$$

which is exactly eq.(A.8), therefore $\eta^{(2)}$ is given asymptotically by (A.18).

From eq.(A.27) we see no η contribution to the $A^{(2)}$ correction, consequently there is no energy conservation at this order. To find the modification to the discrete mode oscillation caused by radiation, we must go to the next order. The third order part of (A.23) is given by

$$\begin{aligned}\ddot{A}^{(3)} + \omega_0^2 A^{(3)} &= (6iq\tilde{R}^2 - 6\frac{\alpha^2}{\omega_0^2} + \frac{a_3}{4})A_0^3 \cos(3\omega_0 t) \\ &+ (2\omega_0\omega^{(2)} + 6iq\tilde{R}^2 A_0^2 + 30\frac{\alpha^2}{\omega_0^2} A_0^2 + \frac{3}{4}a_3 A_0^2)A_0 \cos(\omega_0 t)\end{aligned}\quad (\text{A.30})$$

where $q = 2\sqrt{2}$ and $\tilde{R} = R/A_0^2$ with R given by (A.19). Note the appearance of complex numbers resulting from the coupling of the discrete mode with the imaginary part of the continuum (the real part doesn't contribute at this order). The condition for the resonance term to be absent is

$$\begin{aligned}\omega^{(2)} &= -(30\frac{\alpha^2}{\omega_0^2} + \frac{3}{4}a_3 + 6iq\tilde{R}^2)\frac{A_0^2}{2\omega_0} \\ &= -(0.176 + i0.010)A_0^2\end{aligned}\quad (\text{A.31})$$

The second order real correction to the frequency is negative, so the period of the discrete mode oscillation is greater than $2\pi/\omega_0$. This effect is confirmed by Fig. 6 where we see a longer period at earlier times, when the discrete mode amplitude is large. The imaginary correction to the frequency implies a decay of the amplitude, the effect we are seeking, which in turn means that the real frequency increases with time. The decay rate of the amplitude is given by

$$\frac{dA_0}{dt} = -0.010 A_0^3 \quad (\text{A.32})$$

which is equivalent to (A.21). Fig. 11 shows the evolution of $\phi(x, t)$ calculated numerically with initial data $\phi(x, t) = \phi_K(x) + \eta_D(x)$, so $A_0(0) = 1$. The dashed line shows the amplitude calculated up to the second-order, and including the frequency correction (A.31). The decay of the amplitude of the discrete mode is thus seen to be well approximated by (A.22).

References

- [1] Ames W F 1992 *Numerical Methods for Partial Differential Equations*, 3rd edn, (Academic Press, Boston)
- [2] Arnold V I 1978 *Mathematical Methods of Classical Mechanics* (Springer-Verlag, New York)
- [3] Atiyah M F and Manton N S 1993 Geometry and kinematics of two Skyrmions *Commun. Math. Phys.* **153** 391-422
- [4] Balitsky I I and Yung A V 1986 Collective coordinate method for quasizero modes *Phys. Lett.* **168B** 113-119; Yung A V 1988 Instanton vacuum in supersymmetric QCD *Nucl. Phys.* **B297** 47-85

- [5] Campbell D K, Schonfeld J F and Wingate C A 1983 Resonance structure in the kink-antikink interactions in ϕ^4 theory *Physica* **9D** 1-32
- [6] Demoulini S and Stuart D 1995 *Gradient Flow of the Superconducting Ginzburg-Landau Functional on the plane* U.C.Davis preprint
- [7] Hale J K, Magalhaes L T and Oliva W M 1983 *Introduction to Infinite Dimensional Dynamical Systems-Geometric Theory*, Applied Math. Sciences **47** (Springer-Verlag, New York)
- [8] Landau L D and Lifshitz E M 1976 *Mechanics*, 3rd edn, Chapter 5, (Pergamon Press, Oxford)
- [9] Manton N S 1979 An effective Lagrangian for solitons *Nucl. Phys.* **B150** 397-412
- [10] Manton N S 1982 A remark on the scattering of BPS monopoles *Phys. Lett.* **110B** 54-56
- [11] Manton N S 1988 Unstable manifolds and solitons dynamics *Phys. Rev. Lett.* **60** 1916-1919
- [12] Rajaraman R 1992 *Solitons and Instantons in Quantum Field Theory*, (North-Holland Publ. Co., Amsterdam)
- [13] Segur H 1983 Wobbling kinks in ϕ^4 and sine-Gordon theory *J. Math. Phys.* **24** 1439-1443
- [14] Stuart D 1994 Dynamics of the Abelian Higgs vortices in the near Bogomolny regime *Commun. Math. Phys.* **159** 51-91; Stuart D 1995 The geodesic approximation for the Yang-Mills-Higgs equations *Commun. Math. Phys.* **166** 149-190
- [15] Waindzoch T and Wambach J 1996 *Stability of the B=2 hedgehog in the Skyrme model* to appear in *Nucl. Phys. A*

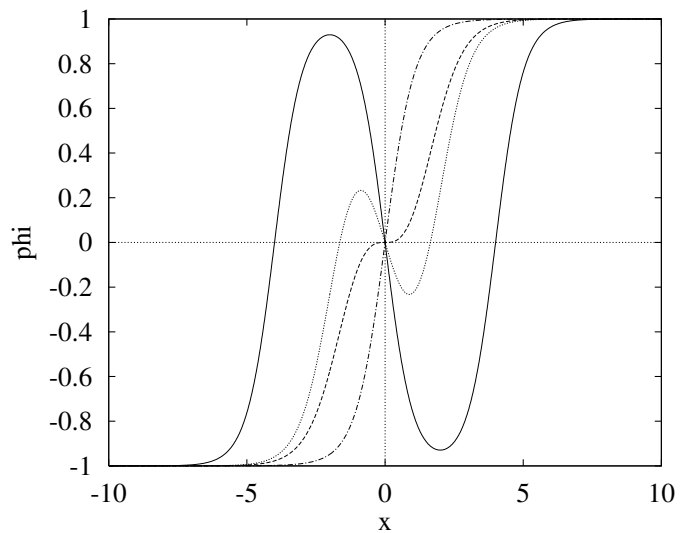


Figure 1: The gradient flow annihilation process for the $K\bar{K}K$ system at time 0 (solid), 59 (dotted), 59.64 (dashed) and 61 (dashed dotted).

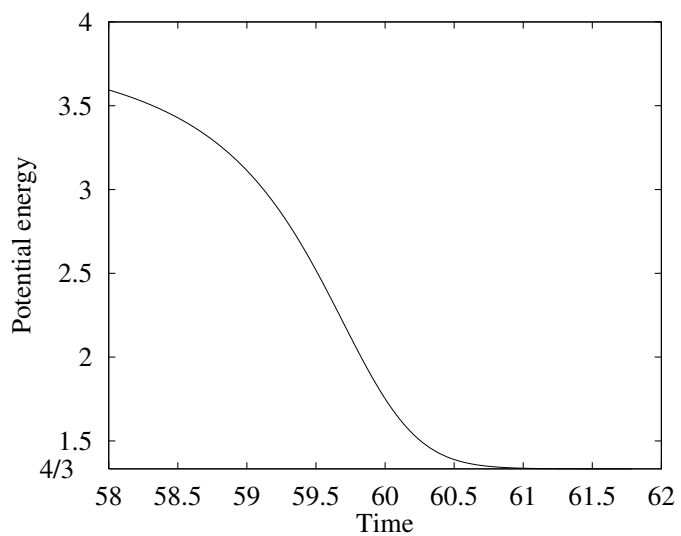


Figure 2: Time dependence of the potential energy along the gradient flow curve.

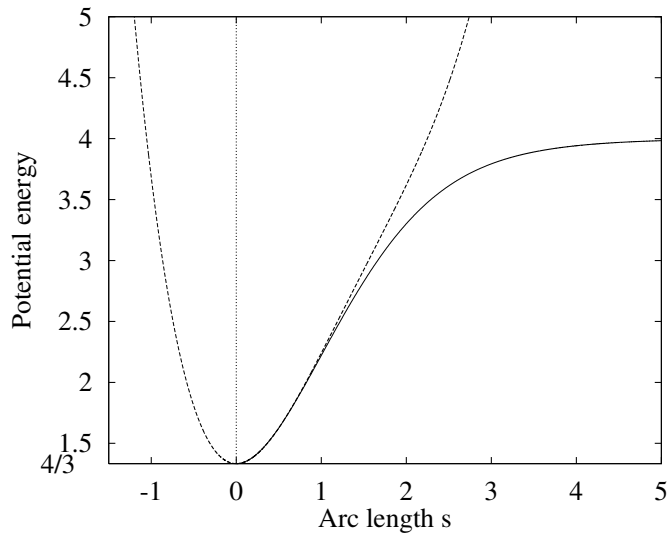


Figure 3: Arc length dependence of the potential energy in the valley. Gradient flow (solid) and discrete mode results for $s < 0$ (the discrete mode result for $s > 0$ is also shown).

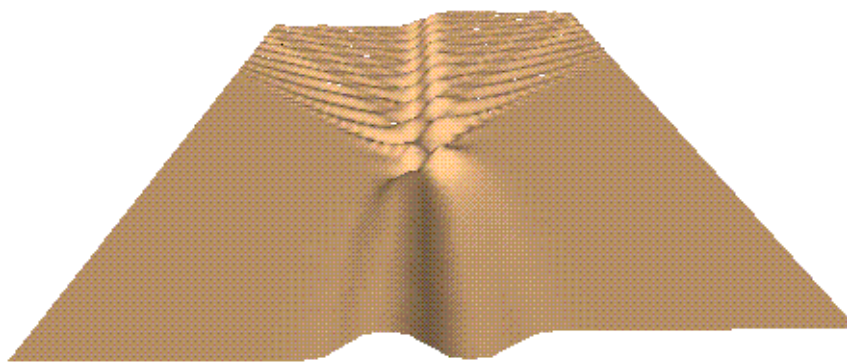


Figure 4: The full dynamics annihilation process.

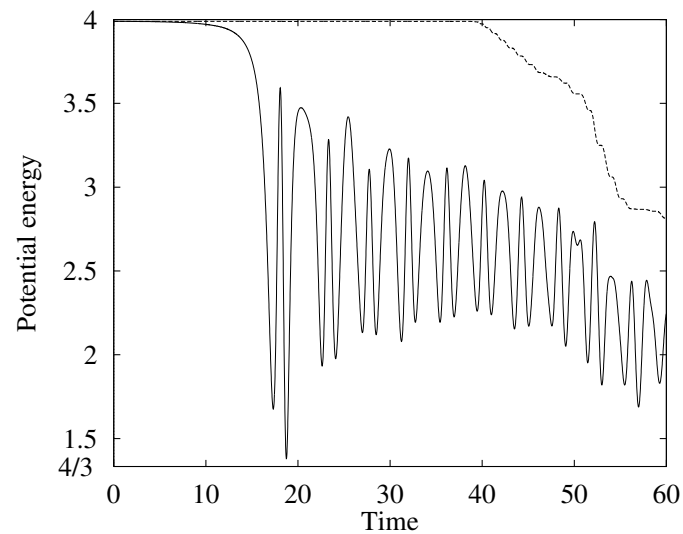


Figure 5: Time dependence of the potential energy (solid) and the total energy (dashed).

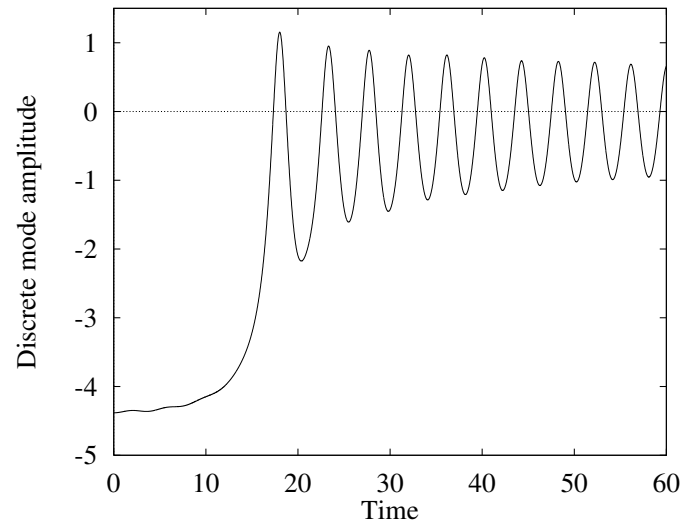


Figure 6: Time dependence of the discrete mode amplitude.

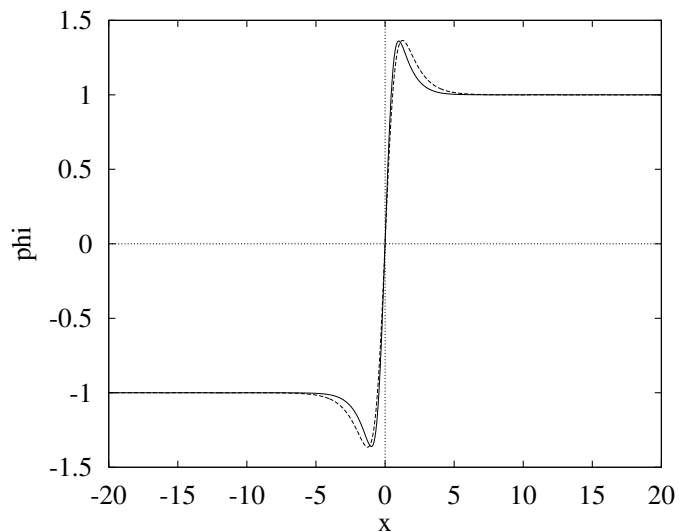


Figure 7: The field ϕ (solid) compared to the discrete mode ansatz at $A = 1.15$ (dashed).

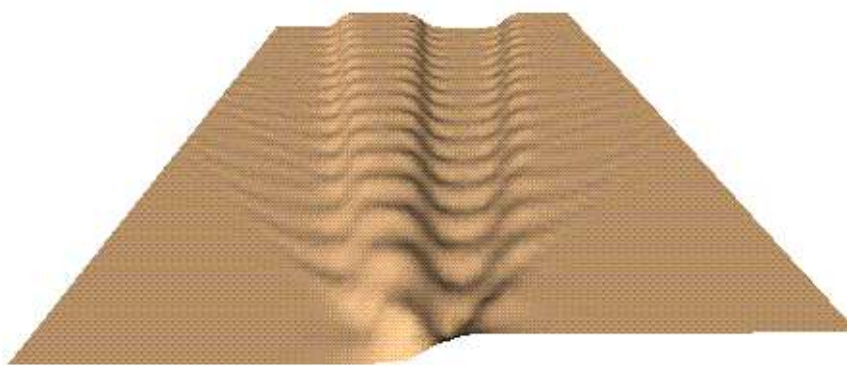


Figure 8: Creation process of three kinks for $C = 3.06$.

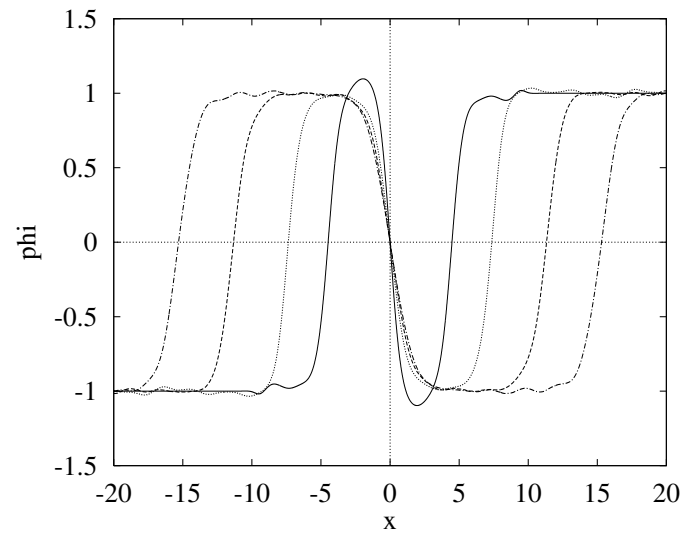


Figure 9: Snapshots of the three kinks creation process at time 10 (solid), 30 (dotted), 60 (dashed) and 90 (dashed dotted).

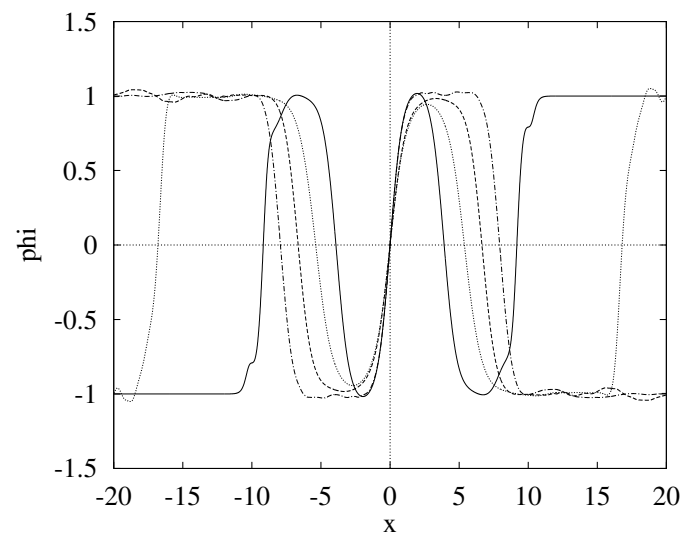


Figure 10: Snapshots of the five kinks creation process at time 10 (solid), 20 (dotted), 40 (dashed) and 60 (dashed dotted).

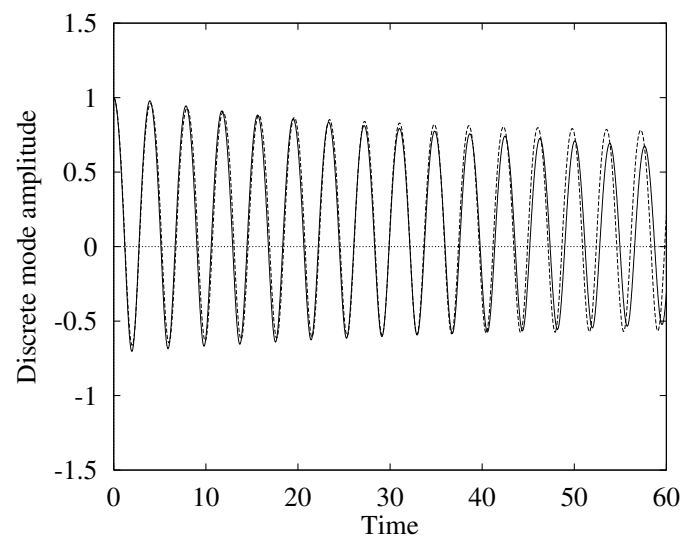


Figure 11: Time dependence of the discrete mode amplitude with $A_0(0) = 1$ (solid) compared to the second order approximation (dashed).